Kinetic Study for the Reactions of Si Atoms with SiH_4

Makoto Koi,[†] Kenichi Tonokura,*[,‡] Atsumu Tezaki,[†] and Mitsuo Koshi[‡]

Department of Mechanical Engineering and Department of Chemical System Engineering, The University of Tokyo, 7-3-1 Hongo, Bunkyo-ku, Tokyo 113-8656, Japan

Received: December 21, 2002; In Final Form: April 15, 2003

Rate constants for the reactions of Si (^{3}P, ^{1}D, and ^{1}S) atoms with SiH_4 have been determined using a combined laser photolysis/laser induced fluorescence technique. The reaction of Si(^{3}P) with SiH_4 is shown to proceed with a rate constant $k(Si(^3P_J) + SiH_4) = (2.1\pm0.2) \times 10^{-10}$ cm^3 molecule^{-1} s^{-1}, with no discernible pressure dependence over a pressure range of 5−20 Torr of N_2 diluent. The rate constants of each triplet component of Si($^3P_{J=0,1,2}$) atoms exhibit no significant spin-orbit dependence within the experimental uncertainties. The results of the density functional theory calculations show that the reaction of Si(^{3}P) atoms with SiH_4 proceeds via a loose transition state. The Si(^{1}D) + SiH_4 reaction rate constant is determined to be $(5.2 \pm 0.3) \times 10^{-10}$ cm^3 molecule^{-1} s^{-1}. The Si(^{1}S) atom is less reactive with SiH_4 than the Si(^{1}D) atom, with an upper limit of $k(Si(^1S) + SiH_4) = 4.7 \times 10^{-13}$ cm^3 molecule^{-1} s^{-1}.

1. Introduction

The reactions of Si atoms with SiH_4 play important roles in chemical vapor deposition (CVD) processes of silicon such as hot-wire CVD (HWCVD) and plasma-enhanced CVD (PECVD).[1−5] Gas-phase products in the chemical reactions are thought to play a critical role in CVD of high-quality amorphous silicon (a-Si:H) and is likely to be important for CVD of polycrystalline silicon as well. Since the ground-state Si(^{3}P) atom is one of the main products in the hot-wire decomposition of SiH_4,[1−4] the information for the rate constant and gas-phase products of the reaction of Si(^{3}P) with SiH_4 is necessary to understand the HWCVD processes of silicon. Since the abundance of electronic excited-state Si(^{1}D) atoms in PECVD is higher than that in HWCVD, reactions related to the Si(^{1}D) atom become important in PECVD processes.[5]

Several experimental and theoretical studies have been performed to examine the reaction mechanism of Si atoms with SiH_4. Tachibana et al.[5] detected Si($^3P_2$) and Si(^{1}D) atoms in a PECVD system using a laser induced fluorescence (LIF) technique and suggested high reactivity of Si atoms with SiH_4. Tanaka et al.[6] measured the reaction rate constants of Si($^3P_2$) and Si(^{1}D) atoms with SiH_4 and the diffusion coefficient for Si(^{1}D) in Ar under radio frequency (RF) silane plasma conditions by using ultraviolet absorption spectroscopy. Woiki et al.[7] studied the reaction of Si($^3P_2$) + SiH_4 at high temperatures using laser flash photolysis combined with the shock tube technique. The temporal profile of Si($^3P_2$) was monitored by atomic resonance absorption spectroscopy, and the rate constant of the Si(^{3}P) + SiH_4 reaction was derived from the kinetic simulation in the system. Takahara et al.[8] determined he rate constant of Si($^3P_1$) + SiH_4 reaction in the 193 nm photolysis of SiH_4/N_2O mixture at 295 K by the LIF detection system. Most recently, cavity ring-down spectroscopy was applied to determine the reaction rate constant of Si(^{3}P) + SiH_4 under DC-operated expanding thermal plasma conditions in which an additional RF pulse was generated to perform time dependent studies.[9]

Sakai et al.[10] studied the mechanism for the insertion of Si(^{3}P) and Si(^{1}D) atoms into the Si−H bond of silane by ab initio quantum chemical calculations, many-body perturbation theory, and a local molecular orbital analysis. Muller et al.[11] studied the possible reaction processes in Si(^{3}P) + SiH_4 reactions by density functional theory calculations and suggested that disilyne (Si_2H_2) is the most favorable product.

$$Si(^3P) + SiH_4 \rightarrow Si_2H_2 + H_2 \qquad \Delta H = -25.1 \text{ kcal mol}^{-1}$$

Figure 1 shows the energy diagram for the Si(^{3}P) + SiH_4 reaction system calculated at the Gaussian-3 (G3)//B3LYP level of theory. In this figure, the most stable isomers of Si_2H_2 for the singlet and triplet states are presented. To our knowledge, there has been no direct detection of final product in the reaction of Si(^{3}P) + SiH_4 in the gas phase.

In the present study, the reaction rate constants of the Si(^3P_J, ^{1}D, and ^{1}S) atoms with SiH_4 are measured by observing temporal decay of Si atoms at 298 K in the pressure range over 5−20 Torr, which provides the basis to understand the silicon CVD processes. The reaction mechanism of Si + SiH_4 reaction is discussed.

2. Experimental Section

Experiments were carried out using a laser-photolysis pump and a LIF probe technique in a quasi-static flow cell (28 mm i.d.). A dye laser (PRA-DL14P) was used as the probe light source. This dye laser was pumped by a frequency-tripled Nd:YAG Laser (Continuum, Surelite-II). The probe UV laser light was generated with a BBO crystal by frequency doubling of the visible dye laser. Mixtures of $SiBr_4$ and SiH_4 diluted in He or in N_2 were flowed in the reaction cell and were irradiated by 193 nm excimer laser (Lamda Physik, COMPex102) pulses coaxially with the flow reactor, where $SiBr_4$ was photolyzed via multiphoton processes to produce Si(^3P_J), Si(^{1}D), and Si(^{1}S) atoms. A typical fluence of the photolysis laser was 70 mJ cm^{-2} per pulse at the observation point. An initial concentration of Si atoms is estimated to be less than 10^{11} molecules cm^{-3}.

* Corresponding author. E-mail: tonokura@reac.t.u-tokyo.ac.jp.
[†] Department of Mechanical Engineering.
[‡] Department of Chemical System Engineering.

10.1021/jp027793r CCC: $25.00
Published on Web 05/24/2003

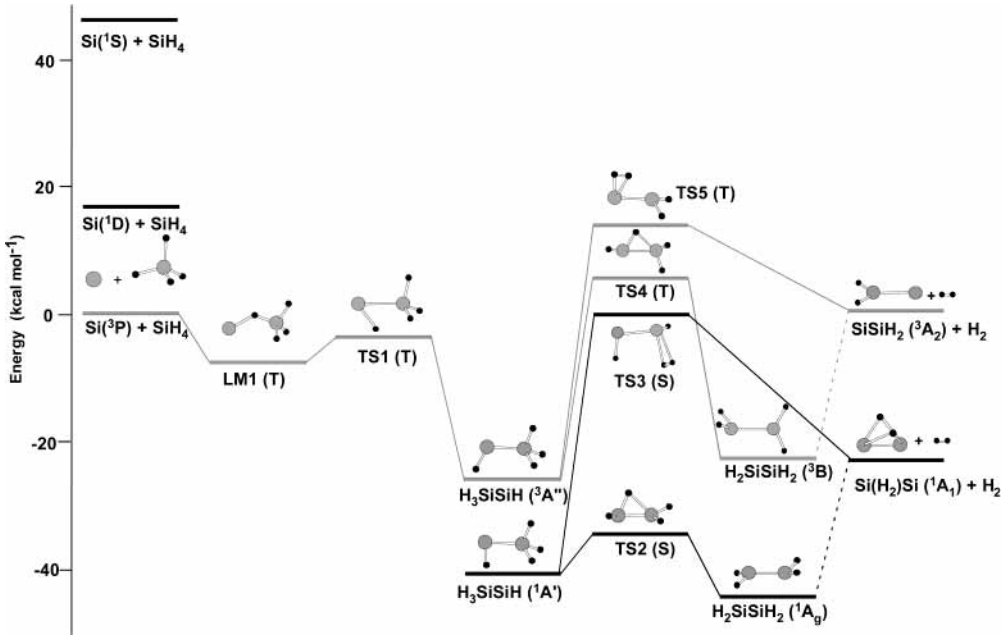

Figure 1. Energy diagram for the reaction of Si(^{3}P) + SiH_4 calculated at the G3//B3LYP/6-31G(d) level of theory.

The transitions 3p4s $^3P_{J'} \leftarrow 3p^2\ ^3P_{J''}$, 3p4s $^1P \leftarrow 3p^2\ ^1D$, and 3p5s $^1P \leftarrow 3p^2\ ^1S$ in the UV region were used to probe Si(^{3}P), Si(^{1}D), and Si(^{1}S) states, respectively. Fluorescence from Si atoms was transmitted through a selected UV band-pass filter (U330), detected by a photomultiplier tube (Hamamatsu, R4220) at right angles to both the photolysis and probe lasers, and then acquired by a boxcar integrator (Stanford Research Systems, SR250) and transferred to a personal computer.

Assuming plug flow condition, the gas residence time between the inlet and the observation point was estimated to be 80 ms at a typical overall flow rate of 300 sccm and 10 Torr total pressure, while the laser was operated at 10 Hz repetition. $SiBr_4$ (Aldrich, 99.995%) was freeze−pump−thaw degassed to remove volatile contaminants, then a 0.5% mixture in He or N_2 diluent was prepared and stored in a glass bulb. The following gases were used without further purification: He (Nippon Sanso, 99.9999%), N_2 (Nippon Sanso, 99.9999%), and SiH_4/He (Nippon Sanso, 1.02%). All the experiments were carried out at room temperature (298 ± 5 K). All indicated error limits for the experimental results are at two standard deviation levels.

The calculations were carried out using the Gaussian 98 series of programs[12] at the Gaussian-3 (G3)//B3LYP level of theory.[13] The initial geometries and zero-point energies were obtained from the B3LYP density functional theory [B3LYP/6-31G(d)].

3. Results

3.1. Generation of Si Atoms. Si(^{3}P), Si(^{1}D), and Si(^{1}S) atoms were produced from the multiphoton dissociation of $SiBr_4$ by the 193 nm excimer laser irradiation.

$$SiBr_4 + nh\nu \rightarrow Si(^3P),\ Si(^1D),\ \text{and}\ Si(^1S) + \text{other products}$$

Logarithmic plots of signal intensity of Si(^{3}P) versus photolysis laser power had a slope of 2−3, indicating that the absorbing species is formed in multiphoton processes. Figure 2 shows the LIF excitation spectrum observed for the ground-state Si(^3P_J) and excited-state Si(^{1}D) and Si(^{1}S) atoms following the 193.3 nm multiphoton dissociation of $SiBr_4$. The six spectral lines correspond to the 3p4s $^3P_{J'} \leftarrow 3p^2\ ^3P_{J''}$ transitions. The spectrum at 253.24 nm is assigned to the 3p5s $^1P \leftarrow 3p^2\ ^1S$ transition. The Si($^1D_2$) atoms were detected by 3p4s $^1P \leftarrow 3p^2\ ^1D$ transition at 288.16 nm.

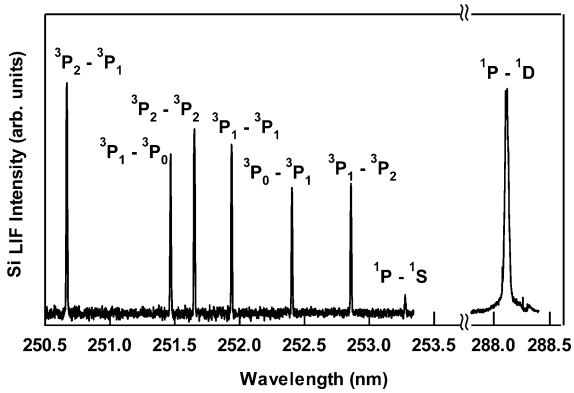

Figure 2. LIF excitation spectrum of Si atoms produced from the 193 nm multiphoton dissociation of $SiBr_4$ in 10 Torr of He diluent.

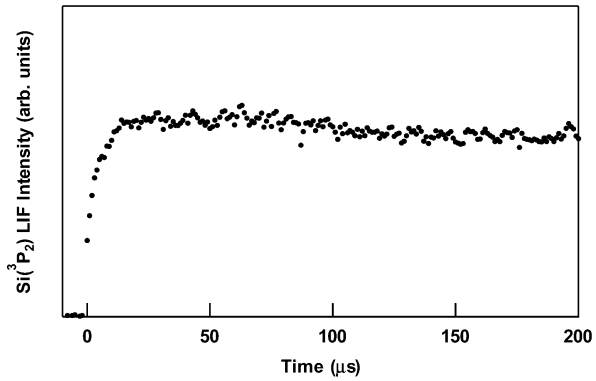

Figure 3. Time profile of Si($^3P_2$) atom from the 193 nm multiphoton dissociation of $SiBr_4$ in 10 Torr of helium diluent at 298 K.

3.2. Rate Constant of Si(^3P_J) + SiH_4. Temporal profiles of Si($^3P_2$) were monitored by 3p4s $^3P_2 \leftarrow 3p^2\ ^3P_2$ transition at 251.61 nm in 10 Torr of He diluent at 298 K. A typical example is shown in Figure 3. There are rise and decay components in the time profile under He buffer conditions. The rise of the

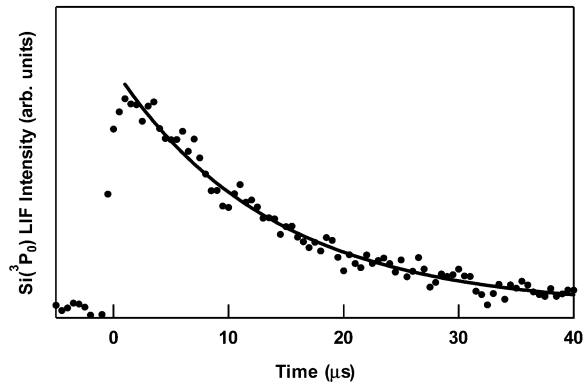

Figure 4. Temporal decay profile of Si(^{3}P$_0$) atom at 10 Torr of N_2 diluent at 298 K.

Si(^{3}P) signal consists of the fast and slow components. The fast rise component results from the direct production in the multiphoton process. The slow rise component is caused mainly by the Si(^{3}P) produced from the electronic quenching of Si(^{1}D) by $SiBr_4$, although the rise time is a little bit faster than the quenching rate of Si(^{1}D) by $SiBr_4$. The collisional removal rates of Si(^{1}D) and Si(^{1}S) by He are $< 1 \times 10^{-15}$ cm^3 molecule^{-1} s^{-1} (ref 14) and $< 1.3 \times 10^{-15}$ cm^3 molecule^{-1} s^{-1} (ref 15), respectively. The rise caused by the electronic quenching of Si(^{1}D) and Si(^{1}S) by He is estimated to 300 μs at 10 Torr of He diluent, and so the quenching of excited-state Si atoms into Si(^{3}P$_J$) states is a small influence on the time profile of Si(^{3}P$_J$).

To avoid the slow formation of Si(^{3}P) atoms, N_2 diluent was used as a buffer gas. The rate for the collisional quenching of Si(^{1}D) to Si(^{3}P) by N_2 is $< 5 \times 10^{-12}$ cm^3 molecule^{-1} s^{-1},[16] and the production rate of Si(^{3}P) from the collisional quenching of Si(^{1}D) by 10 Torr of N_2 was estimated to be 0.6 μs. Figure 4 shows the time profile of Si(^{3}P$_0$) at 10 Torr of N_2 diluent. As shown in this figure, the formation of Si(^{3}P$_0$) atoms proceeds with a time constant of less than 1 μs. The oscillator strength of 0.0732 for the 3p4s ^{3}P$_2$ ←3p^2 ^{3}P$_1$ transition at 250.69 nm is almost same (0.0750) as that for the 3p5s ^{1}P ←3p^2 ^{1}S transition at 253.24 nm.[17] From Figure 2 the production yield of Si(^{1}S) is estimated to be less than one tenth of Si(^{3}P) in the multiphoton dissociation of $SiBr_4$. Therefore, the contribution of the quenching of Si(^{1}S) to the time profile of Si(^{3}P) is negligibly small. Rate constants for the intratriplet relaxation among spin−orbit states by He have been reported to be $k \approx 10^{-12}$ cm^3 molecule^{-1} s^{-1}.[18] The intratriplet relaxation would be fast enough in 10 Torr of N_2 diluent. Hence we used N_2 buffer to determine the reaction rate constant of Si(^{3}P) + SiH_4.

A pseudo-first-order analysis gives the time dependence of the concentration of Si(^{3}P) atoms. The concentration of SiH_4 was varied over the range 1−33 mTorr. The values of k(Si(^{3}P$_J$) + SiH_4) for each spin−orbit J level were obtained from the plot of pseudo-first-order rate constant against [SiH_4]. A typical example for the Si(^{3}P$_1$) atom is shown in Figure 5. The results are summarized in Table 1, along with the statistical uncertainties. The values of k(Si(^{3}P$_J$) + SiH_4) for the spin−orbit J levels are indistinguishable within the experimental uncertainties. The pseudo-first-order loss rate for the reaction of Si(^{3}P) with $SiBr_4$ is estimated to be ca. 1000 s^{-1} from k(Si(^{3}P) + $SiBr_4$) = $(3.3 \pm 0.2) \times 10^{-11}$ cm^3 molecule^{-1} s^{-1} [measured during the present work] and the concentration of $SiBr_4$ (3.3×10^{13} molecules cm^{-3}) used in the present experiments. This value corresponds to a small intercept in the plots shown in Figure 5.

The pressure dependence of k(Si(^{3}P) + SiH_4) was also measured at 5, 10, and 20 Torr of N_2 diluent. The observed

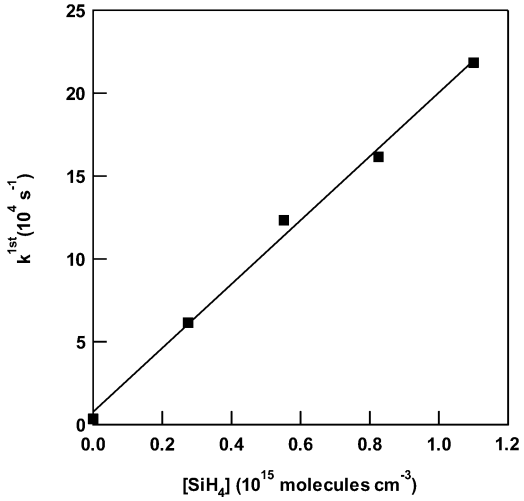

Figure 5. Pseudo-first-order rate constant for the reaction of Si(^{3}P$_1$) atoms with SiH_4 following multiphoton dissociation of $SiBr_4$/SiH_4/N_2 mixtures versus [SiH_4].

TABLE 1: Rate Constant of k(Si(^{3}P$_J$) + SiH_4)

J	k (10^{-10} cm^3 molecule^{-1} s^{-1})	T (K)	ref
0	2.33 ± 0.12	298 ± 5	this work
1	2.13 ± 0.12	298 ± 5	this work
1	4.4 ± 1.0	295 ± 3	ref 8
2	2.07 ± 0.15	298 ± 5	this work
2	3.5 ± 1.0	320−350	ref 6
2	6.6 ± 0.8	1014−1210	ref 7
	1.4 ± 0.6	700 ± 200	ref 9[a]

[a] Spin−orbit state is not specified.

TABLE 2: Pressure Dependence of k(Si(^{3}P) + SiH_4)[a]

P (Torr)	k (10^{-10} cm^3 molecule^{-1} s^{-1})
5	2.07 ± 0.02
10	2.07 ± 0.15
20	1.94 ± 0.08

[a] Si(^{3}P$_1$) atoms were probed.

variation of k(Si(^{3}P) + SiH_4) with pressure is of the order of magnitude of experimental uncertainties and thus is not significant. Consequently, a proposed value of k(Si(^{3}P) + SiH_4) for the pressure range investigated is the average of the values given in Table 2: k(Si(^{3}P) + SiH_4) = $(2.1 \pm 0.2) \times 10^{-10}$ cm^3 molecule^{-1} s^{-1}.

3.3. Rate Constants of Si(^{1}D) + SiH_4 and Si(^{1}S) + SiH_4. The temporal decay profiles of Si(^{1}D) and Si(^{1}S) were measured in 10 Torr of He diluent at 298 K. A typical decay trace recorded for the 3p4s ^{1}P ← 3p^2 ^{1}D transition at 288.16 nm is shown in Figure 6. Experiments were performed at 1 mTorr of $SiBr_4$ and 0−15 mTorr of SiH_4. The temporal decay profile of the Si(^{1}D) atom was well fitted by a single exponential function. Figure 7 shows the plots of the decay rate of Si(^{1}D) and Si(^{1}S) against SiH_4 concentration. Linear least-squares analysis gives k(Si(^{1}D) + SiH_4) = $(5.2 \pm 0.3) \times 10^{-10}$ cm^3 molecule^{-1} s^{-1}. The y-axis intercept shown in Figure 7 is of a magnitude consistent with the pseudo-first order loss rate for the Si(^{1}D) by $SiBr_4$, 46200 s^{-1}, which is derived using the rate constant k(Si(^{1}D) + $SiBr_4$) = 1.4×10^{-9} cm^3 molecule^{-1} s^{-1} [measured during the present work] and 3.3×10^{13} molecules cm^{-3} (1 mTorr) $SiBr_4$. The reaction of Si(^{1}S) atoms with SiH_4 is slow, and the result of linear least-squares analysis gives an upper limit of the rate constant k(Si(^{1}S) + SiH_4) = 4.7×10^{-13} cm^3 molecule^{-1} s^{-1}.

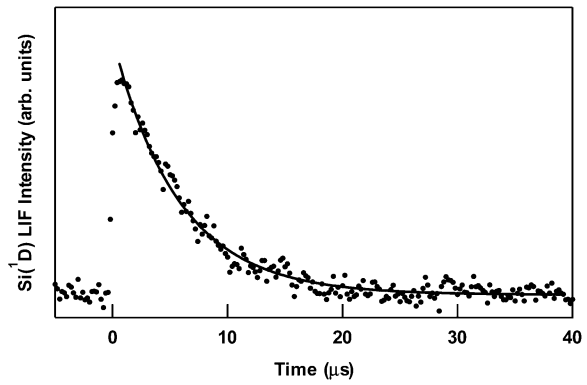

Figure 6. Time profile of Si(^{1}D) atom at 10 Torr of helium diluent at 298 K. [$SiBr_4$] = 3.3 × 10^{13} molecules cm^{-3}, [SiH_4] = 3.0 × 10^{14} molecules cm^{-3}.

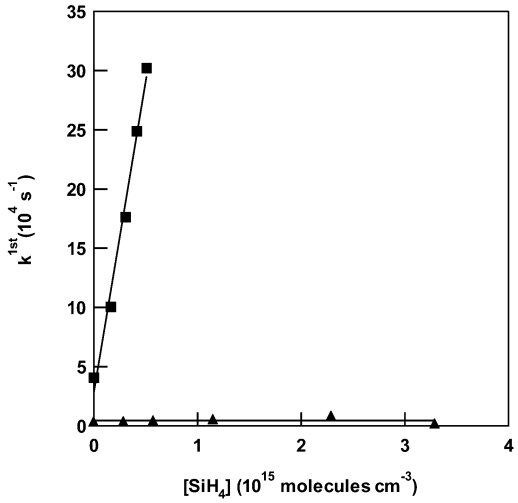

Figure 7. Pseudo-first-order rate constants for the reactions of Si(^{1}D) (squares) and Si(^{1}S) (triangles) with SiH_4 following multiphoton dissociation of $SiBr_4$/SiH_4/He mixtures versus [SiH_4].

Discussion

There have been four previous measurements of k(Si(^{3}P) + SiH_4) in the gas phase (Table 1). Tanaka et al.[6] measured the temporal profiles of Si(^{3}P and ^{1}D) atoms under the RF plasma conditions. They determined k(Si($^3P_2$) + SiH_4) = (3.5 ± 1.0) × 10^{-10} cm^3 $molecule^{-1}$ s^{-1} at the temperature range 320−350 K. Woiki et al.[7] reported a temperature-independent value of k(Si(^{3}P) + SiH_4) = 6.6 × 10^{-10} cm^3 $molecule^{-1}$ s^{-1} between 1040 and 1210 K. Takahara et al.[8] inferred k(Si($^3P_1$) + SiH_4) = (4.4 ± 1.0) × 10^{-10} cm^3 $molecule^{-1}$ s^{-1} at 295 K, which is approximately a factor of 2 larger than that obtained in the present study, k(Si(^{3}P) + SiH_4) = (2.1 ± 0.2) × 10^{-10} cm^3 $molecule^{-1}$ s^{-1}. Takahara et al.[8] monitored the Si(^{3}P) atom using LIF signal at 250.69 nm following the photolysis of an SiH_4/N_2O mixture. In their study, Si atoms were generated by the reaction of O(^{1}D) + SiH_4 and the temporal profiles of Si atoms with rise and decay components were analyzed using a preassumed kinetic model. In the present work, the temporal profile of Si atoms exhibits only a decay component and the pseudo-first-order rate constant is directly obtained from the time profile. Most recently, Hoefnagels et al.[9] determined k(Si(^{3}P) + SiH_4) = (1.4 ± 0.6) × 10^{-10} cm^3 $molecule^{-1}$ s^{-1} at (700 ± 200) K under DC operated expanding thermal plasma conditions. Figure 8 summarizes the rate constants of Si(^{3}P) with SiH_4. It seems that there is no temperature dependence in the temperature range 298−1000 K. The upper limit of the rate constant of Si + SiH_4 reaction estimated from the simple gas-kinetic collision model is $k \approx 10^{-10}$ cm^3 $molecule^{-1}$ s^{-1}. The experimental result of the Si(^{3}P) + SiH_4 system, k = (2.1 ± 0.2) × 10^{-10} cm^3 $molecule^{-1}$ s^{-1}, is consistent with this value, which suggests that the reaction occurs on every collision. The lack of spin−orbit dependence in the rate constants suggests that the intratriplet transition rates in collisions of Si(^3P_J) with N_2 are much faster than the reaction rate of Si(^3P_J) with SiH_4 in the present experimental conditions.

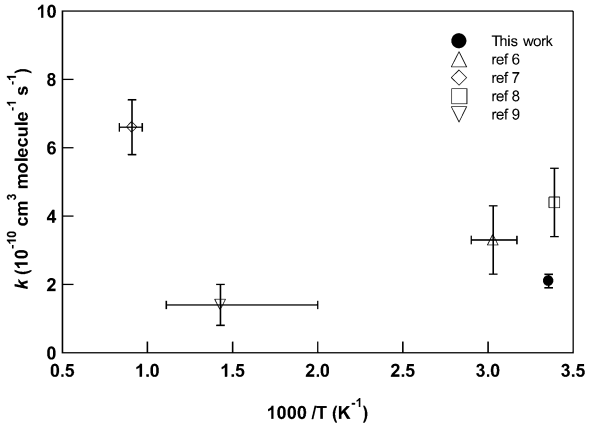

Figure 8. Rate constants of Si(^{3}P) + SiH_4 as a function of temperature.

Sakai et al.[10] found the transition state (TS) for the reaction of Si(^{3}P) + SiH_4 with an activation energy of 7.3 kcal mol^{-1} at the MP4/6-31G(d,p)//HF/6-31G(d) level of theory. On the other hand, the current G3//B3LYP/6-31G(d) calculations show that the reaction of Si(^{3}P) + SiH_4 proceeds via a loose transition state (TS1) with no barrier (−3.6 kcal mol^{-1}). The lack of temperature dependence shown in Figure 8 supports the barrier-free assumption for the reaction of Si(^{3}P) with SiH_4.

The reaction of the O(^{3}P) atom with SiH_4 is a simple H atom abstraction to produce OH + SiH_3 and requires an activation energy of about 10 kcal mol^{-1}.[19] The mechanism of the reaction of Si(^{3}P) with SiH_4 is different from the reaction of O(^{3}P) and it is expected that the reaction is not a simple H atom abstraction. According to the present calculations, the first step of the Si(^{3}P) + SiH_4 reaction is the hydrogen abstraction reaction by Si atom (LM1), and the recombination of SiH and SiH_3 occurs throughout TS1. Triplet silylsilylene is produced via the "near abstraction mechanism". The heat of reaction of triplet silylsilylene formation is predicted to be −23.2 kcal mol^{-1}, the isomerization to triplet disilene via TS4 is unlikely because of a relative energy of 5.5 kcal mol^{-1} above the reactants. It is expected that singlet silylsilylene is produced via an intersystem crossing from triplet silylsilylene without collision. TS3 (0.0 kcal mol^{-1}) directly correlates to disilyne and hydrogen molecules. The isomerization of singlet silylsilylene to singlet disilene occurs with an energy barrier of 7.0 kcal mol^{-1} (TS2). Consequently, disilyne and hydrogen molecules would be produced as final products.

The decay of Si(^{1}D) atoms consists of the reaction and quenching processes with SiH_4. Tanaka et al.[6] determined k(Si(^{1}D) + SiH_4) = (7.4 ± 0.4) × 10^{-10} cm^3 $molecule^{-1}$ s^{-1} around 340 K. Our value of (5.2 ± 0.3) × 10^{-10} cm^3 $molecule^{-1}$ s^{-1} at 298 K is in reasonable agreement with that reported by Tanaka et al.[6] Sakai et al.[10] reported that the reaction mechanism of Si(^{1}D) + SiH_4 is insertion of Si atom into Si−H bond via trans TS geometry with an activation energy of 2.4 kcal mol^{-1} at the MP4/6-31G(d,p)//HF/6-31G(d) level of theory, and the final products of silylsilylene exhibit cis geometry in C_1 symmetry. However, the rate constant of (5.2 ± 0.3) × 10^{-10} cm^3

molecule^{-1} s^{-1} at 298 K suggests no reaction barrier. The reaction of Si(^{1}D) with SiH_4 is faster than the reaction of Si(^{3}P) with SiH_4. It can be explained that the cross section of Si−H insertion of Si(^{1}D) is larger than that of hydrogen abstraction of Si(^{3}P).

The reaction of Si(^{1}S) atoms with SiH_4 is relatively slower than the reaction of Si(^{1}D) which has same spin multiplicity. According to the Russel−Saunders coupling scheme, the total degeneracy of the atomic state is characterized by $g = (2S + 1)(2L + 1)$, where S is the quantum number of the resultant spin angular momentum and L is the quantum number of the resultant orbital angular momentum. There are five degenerated states corresponding to ^{1}D and one state corresponding to ^{1}S. Two electrons are in different 3p orbitals for the three states in the five degenerated states of $^1D_2$ (open singlet), while two electrons are in the same 3p orbital for $^1S_0$ (closed singlet). Since the closed singlet atom cannot insert into the Si−H bond and abstract the H atom, the reactivity is relatively lower than the open singlet atom. The reaction of Si(^{1}S) atom with SiH_4 would be mainly electronic quenching to Si(^{3}P) and Si(^{1}D) states.

Although we surveyed Si_nH_m ($n = 1, 2$; $m = 1-4$) reaction products of Si + SiH_4 reaction using photoionization mass spectrometry, these species were not observed with sufficient signal intensity. Most recently, Maier et al.[20] detected silylsilylene and disilene as a product of the reaction of Si(^{3}P) atom with SiH_4 in solid argon at 10 K. The quantitative measurements for the reaction products are necessary for further discussion of the reaction mechanism.

Conclusions

We have measured the reaction rate constants of Si atoms with SiH_4 molecules at room temperature. The reaction of the Si(^{3}P) atom with SiH_4 is shown to proceed with a rate constant $k(Si(^3P_J) + SiH_4) = (2.07 \pm 0.15) \times 10^{-10}$ cm^3 molecule^{-1} s^{-1}. It seems that the reaction of Si(^{3}P) + SiH_4 is not temperature dependent in the temperature range 298−1000 K. The rate constant for the reaction of singlet Si atoms with SiH_4 is quite different between ^{1}D and ^{1}S states.

References and Notes

(1) Tange, S.; Inoue, K.; Tonokura, K.; Koshi, M. *Thin Solid Films* **2001**, *395*, 42.
(2) Nozaki, Y.; Kongo, K.; Miyazaki, T.; Kitazoe, M.; Hori, K.; Umemoto, H.; Masuda, A.; Matsumura, H. *J. Appl. Phys.* **2000**, *88*, 5437.
(3) Tonokura, K.; Inoue, K.; Koshi, M. *J. Non-Cryst. Solids* **2002**, *229*−*302*, 25.
(4) Tonokura, K.; Koshi, M. *Curr. Opin. Solid State Mater. Sci.* **2002**, *6*, 479.
(5) Tachibana, K.; Mukai, T.; Harima, H. *Jpn. J. Appl. Phys.* **1991**, *32*, L1208.
(6) Tanaka, T.; Hiramatsu, M.; Nawata, M.; Kono, A.; Goto, T. *J. Phys. D Appl. Phys.* **1994**, *27*, 1660.
(7) Woiki, D.; Catoire, L.; Roth, P. *AIChE J.* **1997**, *43*, 2670.
(8) Takahara, A.; Tezaki, A.; Matsui, H. *J. Phys. Chem. A* **1999**, *103*, 11315.
(9) Hoefnagels, J. P. M.; Stevens, A. A. E.; Boogaarts, M. G. H.; Kessels, W. M. M.; van de Sanden, M. C. M. *Chem. Phys. Lett.* **2002**, *360*, 189.
(10) Sakai, S.; Deisz, J.; Gordon, M. S. *J. Phys. Chem.* **1989**, *93*, 1888.
(11) Muller, R. P.; Holt, J. K.; Goodwin, D. G.; Goddard, W. A., III *MRS Symposium Proceedings* **2000**, *609*, A6.1.1.
(12) Frisch, M. J.; Trucks, G. W.; Schlegel, H. B.; Scuseria, G. E.; Robb, M. A.; Cheeseman, J. R.; Zakrzewski, V. Z.; Montgomery, J. A., Jr.; Stratmann, R. E.; Burant, J. C.; Dapprich, S.; Millam, J. M.; Daniels, A. D.; Kudin, K. N.; Strain, M. C.; Farkas, O.; Tomasi, J.; Barone, V.; Cossi, M.; Cammi, R.; Mennucci, B.; Pomelli, C.; Adamo, C.; Clifford, S.; Ochterski, J.; Petersson, G. A.; Ayala, P. Y.; Cui, Q.; Morokuma, K.; Malick, D. K.; Rabuck, A. D.; Raghavachari, K.; Foresman, J. B.; Cioslowski, J.; Ortiz, J. V.; Baboul, A. G.; Stefanov, B. B.; Liu, G.; Liashenko, A.; Piskorz, P.; Komaromi, I.; Gomperts, R.; Martin, R. L.; Fox, D. J.; Keith, T.; Al-Laham, M. A.; Peng, C. Y.; Nanayakkara, A.; Gonzalez, C.; Challacombe, M.; Gill, P. M. W.; Johnson, B.; Chen, W.; Wong, M. W.; Andres, J. L.; Gonzalez, C.; Head-Gordon, M.; Replogle, E. S.; Pople, J. A. *Gaussian 98*, revision A.7; Gaussian, Inc.: Pittsburgh, PA, 1998.
(13) Baboul, A. G.; Curtiss, L. A.; Redfern, P. C.; Raghavachari, K. *J. Chem. Phys.* **1999**, *110*, 7650.
(14) Husain, D.; Norris, P. E. *Chem. Phys. Lett.* **1977**, *53*, 474.
(15) Husain, D.; Norris, P. E. *Chem. Phys. Lett.* **1977**, *51*, 206.
(16) Husain, D.; Norris, P. E. *J. Chem. Soc., Faraday Trans. 2* **1978**, *74*, 1483.
(17) Lide, D. R., Ed.; *CRC Handbook of Chemistry and Physics*, 80th ed.; CRC Press: Boca Raton, FL, 1999; p 10−133.
(18) Le Picard, S. D.; Honvault, P.; Bussery-Honvault, B.; Canosa, A.; Laube, S.; Launay, J.-M.; Rowe, B.; Chastaing, D.; Sims, I. R. *J. Chem. Phys.* **2002**, *117*, 10109.
(19) Buchta, C.; Stucken, D. V.; Vollmer, J. T.; Wagner, H. Gg. *Z. Phys. Chem.* **1994**, *185*, 153.
(20) Maier, G.; Reisenauer, H. P.; Glatthaar, J. *Chem. Eur. J.* **2002**, *8*, 4383.